International Journal of
Nanoscience and Nanotechnology

Research Article 2025, Volume 21, Issue 2

Laser-Assisted Synthesis and Modification of Nanodiamond/Gold Nanocomposites: A Novel Therapeutic Approach for Burn Wound Healing in Diabetic Rats

Fariba MehradNia[1], Batool Sajad[1*], Farideh Bahrami[2], Seyedeh Soraya Mousavi[1], Seyyed Ahad Bagheri[2], Seyyed Homayoun Sadraei[3], Javad Raouf Sarshoori[4]

Received 10 January 2025
Accepted 27 April 2025

DOI: 10.22034/ijnn.2025.2055216.2640

International Journal of Nanoscience and Nanotechnology

Abstract

This study presents a novel laser-assisted method for synthesizing a nanocomposite of nanodiamonds (NDs) and gold nanoparticles (AuNPs). The proposed approach uniquely uses laser treatment to simultaneously create the nanocomposite and modify the ND structure, enhancing its biomedical properties.

The therapeutic potential of this nanocomposite was evaluated in diabetic wound healing studies using highly diabetic rat models, where it demonstrated superior efficacy compared to other treatments. Individual treatments with NDs and AuNPs showed significantly improved outcomes compared to the control group. The ND/AuNP nanocomposite showed higher wound closure rates by Day 7 compared to ND, AuNP, and control groups ($p < 0.001$). Re-epithelialization analysis on Day 21 confirmed superior regeneration in the ND/AuNP group compared to all other groups ($p < 0.001$). These results highlight the promise of our innovative synthesis strategy for advancing therapeutic applications in diabetic wound healing.

Keywords: Nanodiamonds, Gold Nanoparticles, Laser-Assisted Synthesis, Diabetic Wound Healing, Raman Spectroscopy, Nanocomposites

How to cite this article
MehradNia F, Sajad B, Bahrami F, Mousavi SS, Bagheri SA, Sadraei SH, Raouf Sarshoori J. Laser-Assisted Synthesis and Modification of Nanodiamond/Gold Nanocomposites: A Novel Therapeutic Approach for Burn Wound Healing in Diabetic Rats. Int. J. Nanosci. Nanotechnol., 2025;2: 89-96. DOI: 10.22034/ijnn.2025.2055216.2640

1. Introduction

Detonated nanoscale diamond particles emerged in the 1960s. They have high stability and are biocompatible, making them useful for quantum technologies. Gold nanoparticles (AuNPs) are known for their strong absorption in the visible region, leading to various applications in sensors, solar cells, medical treatments, and catalysts [1-3].

The pulsed laser ablation (PLA (for synthesizing gold nanoparticles offers distinct advantages over conventional methods, including elimination of reducing agents, production of high-purity nanoparticles without subsequent purification steps, and simplification of the process. Combining these unique nanomaterials with carbon-based materials results in a composite with distinct characteristics tailored for specific applications, including drug delivery, biomedicine, cancer imaging, disease detection, electro-mechanics, and nanotechnology [4-7].

Despite the promising applications of nanodiamonds and gold nanoparticles in wound healing, a significant gap exists in understanding their combined effects as a nanocomposite.

While individual properties, such as the antibacterial efficacy of gold nanoparticles and the biocompatibility of nanodiamonds, have been extensively studied, their synergistic effects on diabetic wound healing remain underexplored.

Existing synthesis methods often involve harmful chemicals, highlighting the need for safer physical methods like pulsed laser ablation to produce high-quality nanocomposites.

Given the challenges of healing diabetic wounds stemming from compromised blood flow, it is essential to identify new composites that exhibit antimicrobial and healing properties.

Gold nanoparticles, for instance, have been shown to

[1] *Department of Atomic and Molecular Physics, Faculty of Physics, Alzahra University, Tehran, Iran*

[2] *Department of Physiology and Medical Physics, Faculty of Medicine, Baqiyatallah University of Medical Sciences, Tehran, Iran*

[3] *Department of Anatomy, Faculty of Medicine, Baqiyatallah University of Medical Sciences, Tehran, Iran*

[4] *Department of Anatomy, Faculty of Medicine, Baqiyatallah University of Medical Sciences, Tehran, Iran*

E-mail: bsajad@alzahra.ac.ir

enhance biochemical processes involved in skin repair and promote collagen production, making their combination with nanodiamonds particularly relevant for improving patient outcomes [2, 4, 6].

The present study introduces a laser-assisted approach for synthesizing a nanocomposite of nanodiamonds (NDs) and gold nanoparticles (AuNPs) with enhanced spectral properties.

The method comprises two laser-based steps: the first produces gold nanoparticles through laser ablation, and the second forms the nanocomposite by irradiating a mixture of NDs and AuNP suspensions. This purely physical synthesis route avoids the complications associated with chemical methods. Such conventional routes for nanocomposites often involve toxic reagents, poor reproducibility, and multi-step procedures that increase both cost and environmental impact. In contrast, laser-assisted synthesis enables rapid and clean production of nanoparticles without chemical residues, offering superior control over particle size and dispersion [8].

The synthesized nanocomposite was evaluated for treating burn wounds in diabetic rats with severe hyperglycemia (blood glucose levels exceeding 400 mg/dL).

The findings demonstrate that wounds treated with the ND-AuNP composite showed significantly improved wound closure and re-epithelialization compared to treatments using either gold or diamond nanoparticles alone.

These results underscore the potential of this innovative composite for advanced wound care, particularly for diabetic patients, while mitigating the risks associated with chemical synthesis residues.

What distinguishes this study is the dual-function laser-based approach, which integrates gold nanoparticle synthesis and subsequent nanocomposite formation in a purely physical, sequential manner—an aspect not yet reported in similar wound healing studies [9].

2. Materials and Methods

2.1. Materials

Materials used for synthesis included a gold plate (99.99% purity, Swiss fine gold) and nanodiamond particles (5-6 nm average size) supplied by the Shano Sci group.

2.1.1. Synthesis of Gold Nanoparticles

Gold nanoparticles were produced through laser ablation using a Q-switched Nd:YAG laser (wavelength: 1064 nm, pulse duration: 9 ns, repetition rate: 1–10 Hz). The laser parameters and dimensions were optimized based on previous studies [10-12]. During ablation, the liquid in the cuvette was rotated at 400 rpm to prevent crater formation on the gold plate. The resulting gold nanoparticle concentration was 90–100 ppm.

2.1.2. Preparation of Nanodiamond Suspension

A stable nanodiamond suspension was prepared by adding NDs to a 37% hydrochloric acid solution, followed by ultrasonic treatment and heating to 90°C, achieving a density of $\approx 10^{13}$ particles/cm³.

The detonation-nanodiamond aggregates were treated with a 3:2 (v/v) mixture of distilled water and concentrated hydrochloric acid (37%), giving an effective working concentration of ≈15% w/w (≈5 M), below the HCl–water azeotrope (~20.2%). After 20 min of ultrasonic homogenization, the vessel was sealed to prevent vapor escape and heated indirectly in a boiling-water bath (100 °C; solution temperature ≈90 °C) for 1 h. Because the vessel was sealed, no HCl was lost, and no corrosive vapor was released during heating, the elevated temperature neither altered the acid concentration nor posed the hazards associated with heating a volatile acid in an open system. Under these mild, closed conditions, the dilute acid dissolves residual metallic impurities. At the same time, the combined ultrasonic/thermal treatment deaggregates the nanodiamond clusters, a standard, safe route for purifying and deaggregating detonation nanodiamonds.

2.1.3. Nanocomposite Formation

The nanocomposite was then formed by mixing laser-ablated AuNPs with the optimized ND suspension in a 5:1 volume ratio, stirred at 200 rpm. This mixture was irradiated using the Q-switched Nd:YAG laser (1064 nm, 3.3 Hz repetition rate) for up to an hour. The formation of the nanocomposite was indicated by a color change from milky to pale pink after 30 minutes, with a final particle density of $\approx 10^{12}$ particles/cm³.

2.2. Animals

Thirty-two rats (weight range: 220-270 g) were individually housed in plastic cages under controlled conditions (20-22°C, 12-hour light/dark cycle) with ad libitum access to food and water. Blood glucose levels for all rats exceeded 400 mg/dL. The guidelines for working with laboratory animals, established by the Ethics Committee of Baqiyatallah University of Medical Sciences, were followed according to the IR.BMSU.AEC.1402.042 Ethics Code.

2.3. In-Vivo Experimental Design

Animals were anesthetized via intraperitoneal injection of ketamine (100 mg/kg) and xylazine (10 mg/kg). The dorsal skin was shaved and disinfected with alcohol. Two full-thickness circular second-degree burns were created on each rat's back using a brass rod (15 mm diameter) preheated to 100°C for 15 minutes and applied for 15 seconds.

The rats (n=32) were divided into four groups (n=8 per group): A control group (C), without any treatments; the Au group, which received topical treatment with gold nanoparticles (AuNPs); the ND group,

which received topical treatment with nanodiamonds (NDs); and the NDs/AuNPs group, which was treated topically with a combination of AuNPs and NDs.

In the treatment groups, 0.2 mL of a colloidal solution containing the nanoparticles was applied to each wound using a pipette, and the solution was allowed to remain for 10 minutes to promote the penetration of the nanoparticles into the wound beds.

Treatments were administered daily, with clinical observations recorded throughout the 21-day study period. At each time point (days 3, 7, and 21), tissue samples from predefined subgroups (n = 2-3 rats per subgroup) were collected after euthanasia for histological analysis.

3. Results and Discussion

3.1. Transmission Electron Microscopy of Purified Nanodiamonds

TEM analysis revealed that the modified NDs exhibited particle sizes below 50 nm (Figure 1). The images confirm the successful size optimization of the nanodiamonds.

3.2. Field Emission Scanning Electron Microscopy

Figure 2 depicts the Field Emission Scanning Electron Microscopy (FESEM) analysis to reveal the topographical and elemental characteristics of the nanoparticles.

AuNPs exhibited spherical morphology (Figure 2a, b, and g) with sizes ranging from 8-17 nm (mean: 13 nm), while nanodiamond particles (Figure 2c, d, and h) ranged from 12-24 nm (mean: 19 nm).

The ND/AuNP composite displayed a distinctive cauliflower-like structure, with ND acting as nucleation sites.

Figure 2 (e & f) shows that the gold nanoparticles densely coat the nanodiamond surfaces, resulting in a characteristic cauliflower-like morphology. This structural arrangement not only enhances the surface area available for interactions but may also improve the overall stability and functionality of the

composite in various applications, such as drug delivery systems and advanced wound care treatments.

3.3. Optical Characterization

3.3.1. UV-Visible Spectroscopy

UV-visible spectroscopy was performed on NDs, AuNPs, and the NDs/AuNPs composite (Figure 3). While the ND suspension showed no distinctive absorption peaks, AuNPs exhibited a characteristic localized surface plasmon resonance (LSPR) peak at 522 nm, indicating a 3-30 nm particle size distribution consistent with FESEM observations [13-14].

The NDs/AuNPs composite spectrum showed noticeable differences compared to the pure AuNPs. The LSPR peak showed reduced intensity and underwent a redshift from 522 nm to 551 nm.

These changes indicate nanoparticle aggregation, where surface electrons become delocalized and shared among aggregated clusters, resulting in lower resonance frequencies. The redshift in λ_{max} further confirms the assembly of nanoparticles during composite formation.

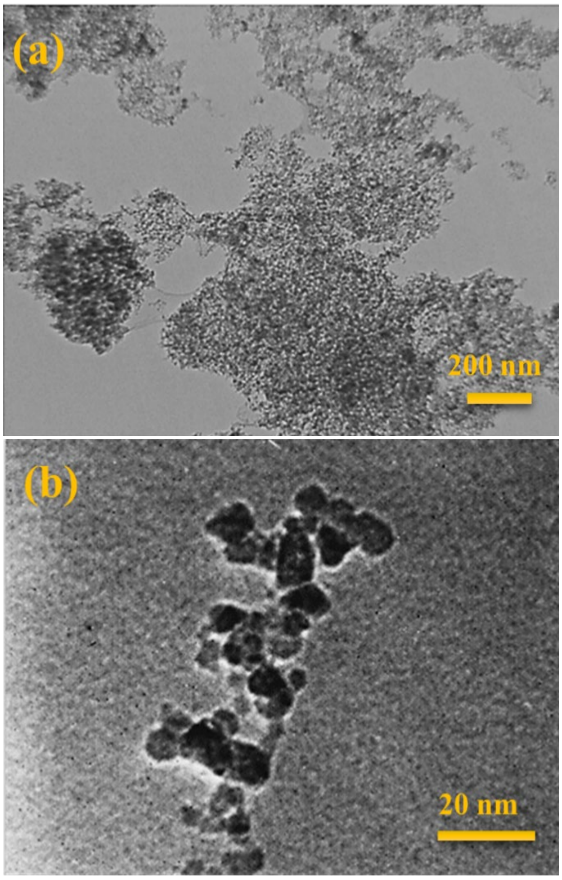

Figure 1. TEM micrographs of nanodiamonds showing (a) unmodified particles with average size of 150-200 nm and (b) optimized particles after size reduction treatment.

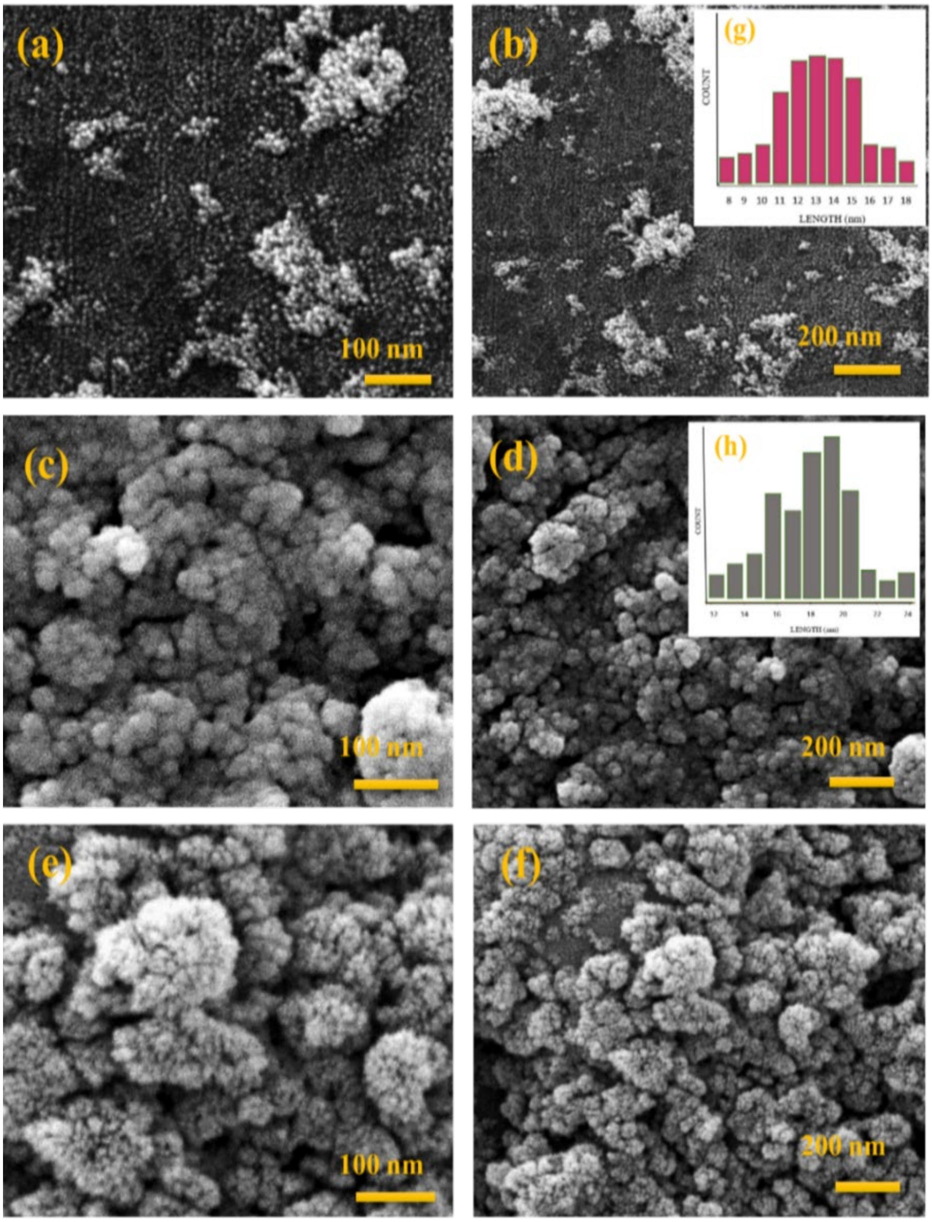

Figure 2. FESEM micrographs of AuNPs (a, b), nanodiamonds (c, d), and NDs/AuNPs nanocomposites (e, f). The insets indicate particle size distribution (g, h).

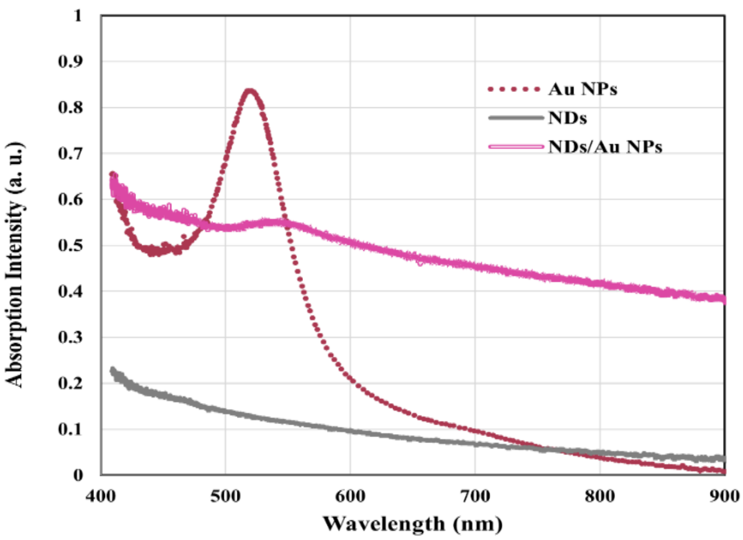

Figure 3. The absorption spectra of AuNPs, NDs, and NDs/AuNPs nanocomposites.

3.3.2. Raman Characterization

The Raman spectrum of AuNPs showed no Raman activity due to their cubic crystal structure and symmetric nature, consistent with previous reports [15]. Figure 4a displays the Raman spectra of the NDs and NDs/AuNPs composite excited at a 532 nm wavelength.

Both samples revealed characteristic features of monocrystalline diamond structure, oxidative groups, and nitrogen-vacancy (NV) centers.

Notably, the strong peak occurring at 475 cm^{-1} is attributed to Raman scattering by acoustic phonons of a distorted diamond lattice [16].

The ND spectrum exhibits a distinct peak at 1325 cm^{-1} assigned to diamond. A sharp and intense band suggests a monocrystalline structure in diamonds. The spectrum further shows an intense peak at 2117 cm^{-1}, attributed to C≡C stretching in the detonation NDs structure, and a significant peak at 2434 cm^{-1}, corresponding to the second-order Raman band characteristic of an ideal diamond lattice [17-18]. The NDs/AuNPs composite formation (Figure 4b) exhibits peaks at distinct wavenumbers.

The NDs/AuNPs composite spectrum shows a weak peak in the 365-430 cm^{-1} region, attributed to Au-C covalent bond stretching vibrations [18-21].

Notable spectral enhancements were observed in the 1560-1718 cm^{-1} range, corresponding to carboxyl group vibrations. These peaks and additional signals at 1718 cm^{-1} and 1762 cm^{-1} confirm effective binding between AuNPs and carboxylate groups [18-21].

3.4. Effect of ND/AuNPs, ND, AuNPs Groups on Wound Closure

Gold nanoparticles (AuNPs) enhance collagen deposition and promote fibroblast proliferation, which are essential for remodeling the extracellular matrix and forming granulation tissue during the healing process. Additionally, they exhibit anti-inflammatory and antioxidant properties, helping to mitigate chronic inflammation associated with diabetic wounds [22, 23]. Nanodiamonds are attractive for drug nanoformulations due to their small size, biocompatibility, and non-toxicity. They enhance the stability and dispersion of drugs while accelerating wound healing without damaging normal tissues. NDs effectively manage inflammation, boost bioactivity, and reduce bacterial attachment and growth. AuNPs serve as antioxidants by preventing the release of reactive oxygen species (ROS) and facilitating the transcutaneous co-delivery of other therapeutics.

In studies involving Wistar Albino rats, AuNPs improved collagen deposition, granulation tissue formation, re-epithelialization, and expedited wound closure. They also inhibited the activity of *P. aeruginosa* and *S. aureus*,

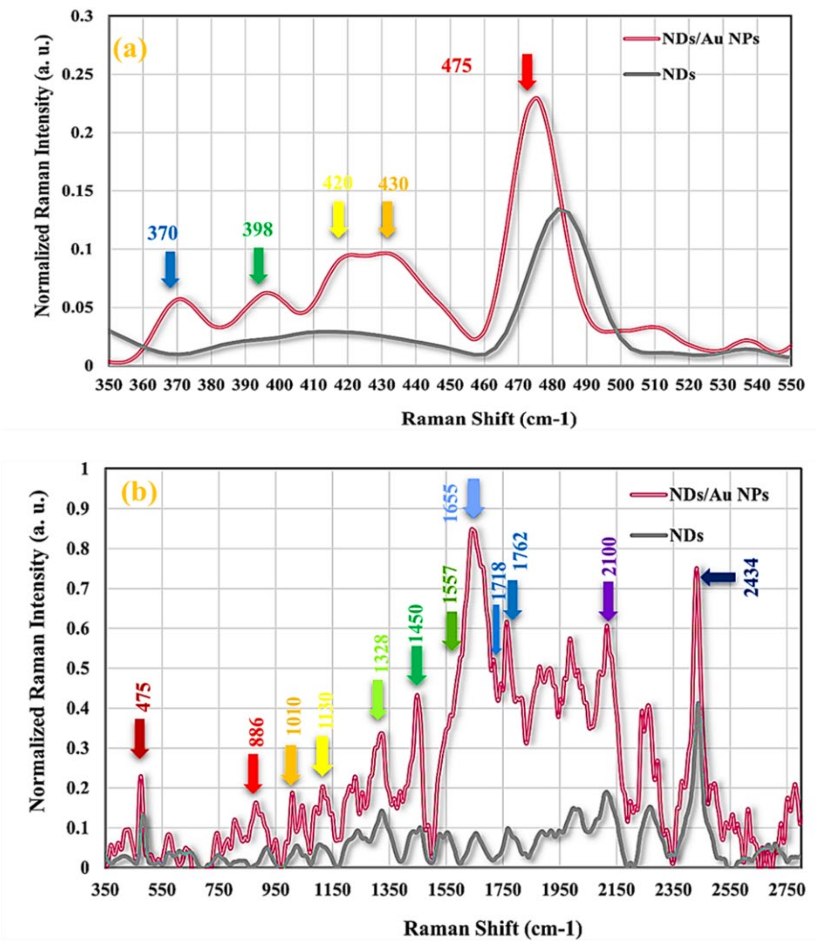

Figure 4. (a) A Comparison between the normalized Raman spectra of NDs, and NDs/AuNPs. (b) A Comparison between the normalized Raman spectra of NDs and NDs/AuNPs at lower Raman shifts.

disrupting their energy metabolism and impairing the function of ATP synthase [24, 25].

The synthesized nanoparticles and their composite were evaluated for wound-healing efficacy in a rat model of diabetic burns. The therapeutic potential was assessed by quantitatively analyzing wound closure rates across different treatment groups.

The comparison of wound closure among the groups on Days 3, 7, and 21 (expressed as percentages) is presented in Table 1.

Analysis of Day 3 data revealed significant differences in wound closure percentages among treatment groups (p=0.016). The ND/AuNP composite group showed significantly enhanced wound closure compared to other groups, with the most pronounced difference observed against the untreated control group. These results demonstrate the superior wound-healing efficacy of the ND/AuNP composite treatment (Figure 5).

By Day 7, wound closure analysis showed highly significant differences among groups (p<0.001). The evidence clearly illustrated that all treatment groups (ND/AuNP composite, ND, and AuNP) demonstrated significantly enhanced wound closure compared to the control group (p<0.001 for each comparison), supporting the therapeutic efficacy of these nanomaterial-based treatments. By day 21, the findings demonstrated that wound closure rates were significantly higher in the diamond and gold nanoparticle combination compared to diamond-only treatment (p=0.014). This remarkable improvement in healing progression represents a crucial milestone in advanced wound therapeutics and could pave the way for developing a new generation of effective combination therapies.

3.5. Effect of ND/AuNPs, ND, and AU-NPs Groups on Re-Epithelization

Analysis of day 3 data revealed no statistically significant differences in re-epithelialization among the treatment groups (Figure 6). It indicates that during the initial phase of wound healing, none of the nanoparticle interventions - whether diamond, gold, or combination-produced distinguishable effects on epithelial regeneration.

By day 7, significant differences in epithelial regeneration emerged among the groups (p = 0.01). The ND/AuNP-treated group showed enhanced epithelial regeneration compared to both AuNP (p = 0.03) and control (p = 0.01) groups. Furthermore, the ND group demonstrated significantly higher epithelial regeneration than the control group (p = 0.03). These results indicate that the ND/AuNP combination most effectively promotes epithelial regeneration among the tested interventions.

The ND group showed significantly higher epithelial regeneration than the control group (p = 0.03). By Day 21, the differences among groups remained statistically significant (p < 0.001).

The nanodiamond/gold group exhibited a substantial enhancement in epithelial regeneration when compared to both the diamond group (p = 0.01) and the gold group (p = 0.01), as well as a significant improvement over the control group (p < 0.001). This consistent trend underscores the effectiveness of the nanodiamond/gold treatment in facilitating epithelial regeneration over time.

The comparison of re-epithelialization among the groups on Days 3, 7, 14, and 21 is summarized in Table 2.

In addition, significant differences were observed in the diamond group compared to the control group (p = 0.005) and in the gold group compared to the control

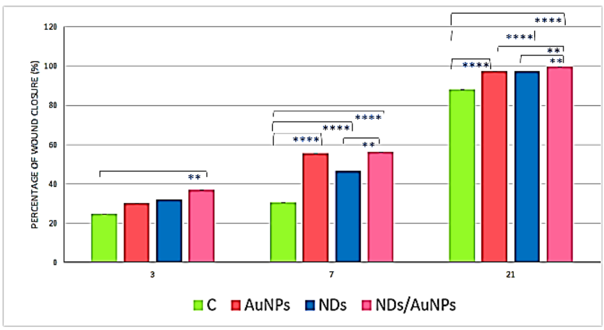

Figure 5. Comparison of wound closure among groups on days 3, 7 and 21 Data are presented as mean ± SD. Statistical significance is indicated by asterisks (*p ≤ 0.05, **p ≤ 0.01, ***p ≤ 0.001).

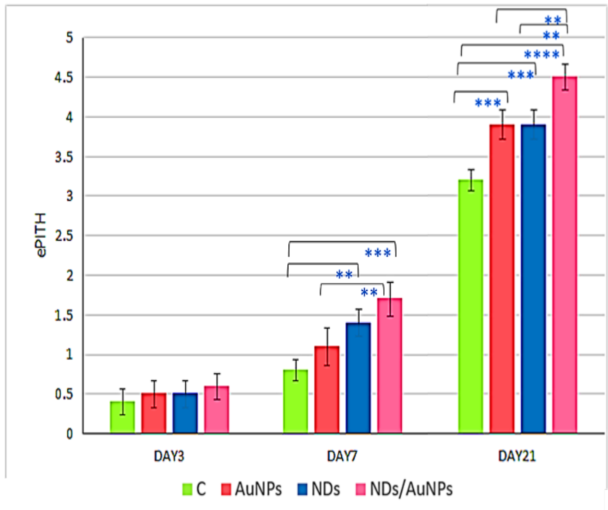

Figure 6. Comparison of re-epithelialization between groups on days 3, 7, and 21. Data are presented as mean ± SD. Statistical significance is indicated by asterisks (*p ≤ 0.05, **p ≤ 0.01, ***p ≤ 0.001).

Table 1. Comparison of wound closure observation between groups on Days 3, 7 and 21 (data are shown as %).

Wound closure percentage Average (%)	Groups				P value
Days	Control	AuNPs	NDs	NDs/AuNPs Composite	
3	24.62	29.89	31.78	36.82	0
7	30.19	55.47	46.44	55.94	0
21	88	97.21	97.28	99.41	0

Table 2. Comparison of re-epithelialization among groups on Days 3, 7, 14, and 21.

Re-Epithelialization	Groups				P value
Days	Control	AuNPs	NDs	NDs/AuNPs Composite	
3	0.4 ± 0.51	0.5 ± 0.52	0.5 ± 0.52	0.51 ± 0.6	0
7	0.8 ± 0.42	1.1 ± 0.73	1.4 ± 0.51	1.7 ± 0.67	0
14	1.8 ± 0.42	2.8 ± 0.63	2.7 ± 0.48	3.2 ± 0.42	0
21	3.2 ± 0.42	3.9 ± 0.56	3.9 ± 0.56	4.5 ± 0.52	0

group (p = 0.005). The synthesized ND/AuNP composite exhibits promising properties that may enhance wound healing compared to other commonly used nanoparticles.

As a comparison, silver nanoparticles (AgNPs), with their strong antibacterial characteristics extensively documented in the literature, have effectively inhibited a wide range of bacterial strains; however, their toxicity to mammalian cells and potential environmental risks limit their clinical application [11, 26]. In contrast, our ND/AuNP composite combines the antibacterial properties of gold nanoparticles with the biocompatibility of nanodiamonds, thereby reducing the potential of cytotoxicity while maintaining effective antimicrobial action.

Another example is zinc oxide nanoparticles (ZnONPs). The potential of wound healing is linked to their ability to enhance fibroblast proliferation and migration [27]. However, their effective concentration often poses challenges due to associated cytotoxicity [28]. Furthermore, while ZnONPs have shown effectiveness in enhancing wound healing, their stability and potential for aggregation in biological systems can reduce their applicability [28].

Additionally, the high reactivity of ZnONPs may lead to unpredictable interactions in vivo, resulting in adverse biological responses [29].

In contrast, our ND/AuNP composite mitigates these limitations by integrating the properties of less toxic materials and offering a more favorable safety profile [30, 31]. The results from our study suggest that the ND/AuNP composite not only improves wound closure and re-epithelialization but also reduces the risks associated with more traditional nanoparticle treatments, positioning it as a promising alternative for advanced wound care.

While nanotechnology holds immense clinical promise, several limitations hinder its safe integration into healthcare. Scalability is a significant obstacle, as current small-batch production methods struggle to translate into large-scale manufacturing required for widespread clinical use, as noted by Gunter [32]. Toxicity is another relevant concern in the clinical applications of nanotechnology. Nanoparticles' biocompatibility must be carefully evaluated to ensure patient safety.

must be carefully evaluated to ensure patient safety. The toxicity of nanomaterials significantly depends on their size, shape, and surface chemistry. Comprehensive studies assessing the long-term impacts of nanomaterials on human health and their interactions with biological systems are essential to address these risks [33]. Regulatory issues also pose substantial barriers to adopting nanotechnology in clinical applications. Current regulatory frameworks often lack the specificity needed to adequately address the unique characteristics of nanomaterials, resulting in uncertainty about safety assessments and approval processes [12].

Addressing these limitations is vital for realizing the promise of nanotechnology in healthcare and advancing the development of innovative diagnostic and therapeutic solutions.

4. Conclusion

This study presents a novel laser-assisted approach for the synthesis of nanodiamond/gold nanoparticle (ND/AuNP) nanocomposites with unique structural properties. Extensive characterization was performed by TEM and FESEM confirmed the composite's successful synthesis and unique morphology, highlighting smaller particle sizes and a distinct cauliflower-like structure that enhances its functional properties. Raman analysis indicates the formation of novel bonding interactions between the gold nanoparticles and the carbon-onion functional groups of the nanodiamonds, as evidenced by the appearance of new spectral peaks. Notably, this process induces structural modifications in the defects of the nanodiamonds. Furthermore, the biocompatibility and non-toxicity of these nanocomposites facilitated thorough in vitro and in vivo evaluations.

In diabetic rat models, the wound-healing efficacy of synthesized ND/AuNP composites was evaluated. On Day 3, the ND/AuNP composite group showed the highest wound closure rates compared to the untreated control group (p = 0.016). By Day 7, all treatment groups (ND/AuNP, ND, AuNP) significantly improved wound closure over controls (p<0.001), with the ND/AuNP composite outperforming the ND-only treatment (p = 0.014).

There were no significant differences in re-epithelialization by Day 3; however, by Day 7, the ND/AuNP group exhibited enhanced epithelial regeneration compared to AuNP and control groups (p = 0.03 and p = 0.01, respectively).

By Day 21, significant differences remained, with the ND/AuNP group demonstrating significantly greater epithelial regeneration ($P < 0.001$). Overall, these results mark a significant breakthrough in wound healing therapeutics, highlighting the individual effectiveness of nanodiamonds and gold nanoparticles and revealing a synergistic effect when combined. This synergy may improve treatment strategies aimed at enhancing tissue regeneration. Future studies should focus on optimizing the nanoparticle synthesis methods, identifying effective dosages, and exploring the interactions of ND/AuNP composites with biological tissues.

Additionally, it is essential to address the limitations of existing studies, including their limited scope and their potential biases, to enhance our understanding of the therapeutic applications of these composites. Expanding research in this area can facilitate the development of innovative nanotechnology-based wound care therapies that promote improved healing outcomes. Future work should focus on large-scale synthesis and preclinical evaluation to translate this technology into clinical settings.

Conflict of Interest

The authors declare that they have no conflict of interest.

References

1. Bokobza L, Bruneel JL, Couzi M. Raman spectra of carbon-based materials (from graphite to carbon black) and of some silicone composites. C. 2015;1(1):77-94. https://doi.org/10.3390/c1010077
2. Zhang H, Chen X, Yin ZQ. Quantum information processing and precision measurement using a levitated nanodiamond. Adv Quantum Technol. 2021;4(8):2000154. https://doi.org/10.1002/qute.202000154
3. Montes-García V, Squillaci MA, Diez-Castellnou M, Ong QK, Stellacci F, Samori P. Chemical sensing with Au and Ag nanoparticles. Chem Soc Rev. 2021;50(2):1269-1304. https://doi.org/10.1039/D0CS01112F
4. Torrisi L, Restuccia N. Laser-generated Au nanoparticles for biomedical applications. IRBM. 2018;39(5):307-312. https://doi.org/10.1016/j.irbm.2018.09.005
5. Correard F, Maximova K, Esteve MA, Villard C, Roy M, Al-Kattan A, et al. Gold nanoparticles prepared by laser ablation in aqueous biocompatible solutions: assessment of safety and biological identity for nanomedicine applications. Int J Nanomedicine. 2014;9:5415-5430. https://doi.org/10.2147/IJN.S65817
6. Havel J, Peña-Méndez EM, Amato F, Panyala NR, Buršíková V. Laser ablation synthesis of new gold carbides: From gold-diamond nanocomposite as a precursor to gold-doped diamonds. Rapid Commun Mass Spectrom. 2014;28(3):297-304. https://doi.org/10.1002/rcm.6783
7. Xiao J, Ouyang G, Liu P, Wang CX, Yang GW. Reversible nanodiamond-carbon onion phase transformations. Nano Lett. 2014;14(6):3645-3652. https://doi.org/10.1021/nl5014234
8. Amendola V, Meneghetti M. Laser ablation synthesis in solution and size manipulation of noble metal nanoparticles. Phys Chem Chem Phys. 2009;11(20):3805-3821. https://doi.org/10.1039/b900654k
9. Kautek W, Krüger J, Lenzner M. Laser-assisted synthesis of nanomaterials: Fundamentals and applications. Adv Opt Technol. 2018;7(1):17-29.
10. Dudhane AA, Waghmode SR, Dama LB, Mhaindarkar VP, Sonawane A, Katariya S. Synthesis and characterization of gold nanoparticles using plant extract of Terminalia arjuna with antibacterial activity. Int J Nanosci Nanotechnol. 2019;15(2):75-82.
11. Dinç B. Comprehensive toxicity assessment of silver nanoparticles on Bacteria, human vein endothelial cells, and Caenorhabditis elegans. Results Chem. 2025;14:102092. https://doi.org/10.1016/j.rechem.2025.102092
12. Kumar CSSR, Weissleder R. Regulatory challenges for nanomaterials in medicine: Insights and perspectives. Nat Nanotechnol. 2021;16(8):800-811.
13. Habib A, Tabata M, Wu YG. Formation of gold nanoparticles by Good's buffers. Bull Chem Soc Jpn. 2005;78(2):262-269. https://doi.org/10.1246/bcsj.78.262
14. Sylvestre JP, Poulin S, Kabashin AV, Sacher E, Meunier M, Luong JH. Surface chemistry of gold nanoparticles produced by laser ablation in aqueous media. J Phys Chem B. 2004;108(43):16864-16869. https://doi.org/10.1021/jp047134+
15. Mezni A, Dammak T, Fkiri A, Mlayah A, Abid Y, Smiri LS. Photochemistry at the surface of gold nanoprisms from surface-enhanced Raman scattering blinking. J Phys Chem C. 2014;118(31):17956-17967. https://doi.org/10.1021/jp5038188
16. Zaitsev AM. Optical Properties of Diamond: A Data Handbook. Springer Science & Business Media; 2013.
17. Guselnikova O, Svorcik V, Lyutakov O, Chehimi MM, Postnikov PS. Preparation of selective and reproducible SERS sensors of Hg2+ ions via a sunlight-induced thiol-yne reaction on gold gratings. Sensors (Basel). 2019;19(9):2110. https://doi.org/10.3390/s19092110
18. Li H, Kopiec G, Müller F, Nyßen F, Shimizu K, Ceccato M, et al. Spectroscopic evidence for a covalent sigma Au-C bond on Au surfaces using 13C isotope labeling. JACS Au. 2021;1(3):362-368. https://doi.org/10.1021/jacsau.0c00108
19. He XN, Gao Y, Mahjouri-Samani M, Black PN, Allen J, Mitchell M, et al. Surface-enhanced Raman spectroscopy using gold-coated horizontally aligned carbon nanotubes. Nanotechnology. 2012;23(20):205702. https://doi.org/10.1088/0957-4484/23/20/205702
20. Ma Y, Huang Z, Li S, Zhao C. Surface-enhanced Raman spectroscopy on self-assembled Au nanoparticles arrays for pesticides residues multiplex detection under complex environment. Nanomaterials (Basel). 2019;9(3):426. https://doi.org/10.3390/nano9030426
21. Hong S, Li X. Optimal size of gold nanoparticles for surface-enhanced Raman spectroscopy under different conditions. J Nanomater. 2013;2013:790323. https://doi.org/10.1155/2013/790323
22. Shalaby MA, Anwar MM, Saeed H. Nanomaterials for application in wound healing: current state-of-the-art and future perspectives. J Polym Res. 2022;29:91. https://doi.org/10.1007/s10965-021-02870-x
23. Sheikh-Oleslami S, Tao B, D'Souza J, Butt F, Suntharalingam H, Rempel L, et al. A Review of Metal Nanoparticles Embedded in Hydrogel Scaffolds for Wound Healing In Vivo. Gels. 2023;9(7):591. https://doi.org/10.3390/gels9070591
24. Khalid A, Bai D, Abraham AN, Jadhav A, Linklater D, Matusica A, et al. Electrospun nanodiamond-silk fibroin membranes: a multifunctional platform for biosensing and wound-healing applications. ACS Appl Mater Interfaces. 2020;12(43):48408-48419. https://doi.org/10.1021/acsami.0c15612
25. Wei SC, Chang L, Huang CC, Chang HT. Dual-functional gold nanoparticles with antimicrobial and proangiogenic activities improve the healing of multidrug-resistant bacteria-infected wounds in diabetic mice. Biomater Sci. 2019;7(11):4482-4490. https://doi.org/10.1039/C9BM00772E
26. Shayo GM, Elimbinzi E, Shao GN. Preparation methods, applications, toxicity and mechanisms of silver nanoparticles as a bactericidal agent and superiority of green synthesis method. Heliyon. 2024;10(17):e36539. https://doi.org/10.1016/j.heliyon.2024.e36539
27. Pino P, Bosco F, Mollea C, Onida B. Antimicrobial Nano-Zinc Oxide Biocomposites for Wound Healing Applications: A Review. Pharmaceutics. 2023;15(3):970. https://doi.org/10.3390/pharmaceutics15030970
28. Singh S. Zinc oxide nanoparticles impacts: cytotoxicity, genotoxicity, developmental toxicity, and neurotoxicity. Toxicol Mech Methods. 2019;29(4):300-311. https://doi.org/10.1080/15376516.2018.1553221
29. Kim SB, Na-Kyung Y, Soo-Jin C. Interactions between ZnO Nanoparticles and Polyphenols Affect Biological Responses. Nanomaterials (Basel). 2022;12(19):3337. https://doi.org/10.3390/nano12193337
30. Salesa B, Ferrús-Manzano P, Tuñón-Molina A, Cano-Vicent A, Assis M, Andrés J, et al. Study of biological properties of gold nanoparticles: Low toxicity, no proliferative activity, no ability to induce cell gene expression and no antiviral activity. Chem Biol Interact. 2023;382:110646. https://doi.org/10.1016/j.cbi.2023.110646
31. Gupta C, Prakash D, Gupta S. Cancer treatment with nanodiamonds. Front Biosci (Schol Ed). 2017;9(1):62-70. https://doi.org/10.2741/s473
32. Gunter RM, Sari LK, Hill C. Scalable synthesis of functionalized nanoparticles: Challenges and perspectives. J Nanopart Res. 2023;25(2):45-65.
33. Zhang Y, Sun H, Liu Z. Toxicological profiles of nanomaterials: A comparative analysis. Nano Today. 2022;40:101191.